American Mineralogist, Volume 77, pages 1191–1205, 1992

Substitution of $^{[6,4]}$Al in phlogopite: High-temperature solution calorimetry, heat capacities, and thermodynamic properties of the phlogopite-eastonite join

SUSAN CIRCONE,* ALEXANDRA NAVROTSKY
Department of Geological and Geophysical Sciences, Princeton University, Princeton, New Jersey 08544, U.S.A.

ABSTRACT

Enthalpies of solution of synthetic magnesium aluminum phlogopite samples $K(Mg_{3-X}Al_X)(Al_{1+X}Si_{3-X})O_{10}(OH)_2$ with $0.00 \leq X_{East} \leq 0.92$ were measured in molten $2PbO\text{-}B_2O_3$ at 977 K. The enthalpy of mixing for the phlogopite-eastonite join is large, asymmetric, and endothermic. The solid solution is destabilized more by $^{[6]}$Mg,$^{[4]}$Si substitution into eastonite than by $^{[6]}$Al,$^{[4]}$Al substitution into phlogopite, reflecting the increased strain in the mica structure at high $^{[6,4]}$Al content that arises from increased lateral misfit between the smaller octahedral and larger tetrahedral sheets. The entropy of mixing has been calculated assuming a random distribution of Mg and Al on one octahedral site and a short-range ordered distribution of Al and Si on four tetrahedral sites. The calculated activity-composition relations predict a large region of immiscibility up to ~1500 K that is consistent with observed limits of $^{[6,4]}$Al substitution in naturally occurring Fe-poor phlogopite.

The thermodynamic data for phlogopite and eastonite are assessed using the metastable reaction Phl + 3 Qtz = San + 3 En + H_2O, in which the breakdown of magnesium aluminum phlogopite also produces spinel. A standard enthalpy of formation of phlogopite from the elements at 298 K of -6215.0 ± 3.5 kJ/mol is consistent with both data from high-temperature solution calorimetry and results from phase equilibria experiments. The standard enthalpy of formation of eastonite from the elements at 298 K is between -6352 and -6363 kJ/mol; the large uncertainty arises from estimating the heat capacity of eastonite. The P,T stability of phlogopite increases with increasing $^{[6,4]}$Al content. The equilibrium breakdown of a magnesium aluminum phlogopite with $X_{East} = 0.20$ is shifted up in temperature by 185 K at 5.0 kbar from that of the phlogopite end-member.

INTRODUCTION

Trioctahedral micas commonly occur in igneous and metamorphic assemblages formed over a wide range of pressure, temperature, and chemical composition and act as a reservoir for H_2O in the crust and upper mantle. The breakdown of trioctahedral micas at high pressures and temperatures releases H_2O, forming a hydrous fluid that lowers the temperature at which melting occurs. Well-constrained, internally consistent, and comprehensive thermochemical data for trioctahedral micas are necessary for understanding crustal and upper mantle processes involving melting in the presence of H_2O. However, the available thermochemical data for trioctahedral micas do not encompass the chemical variation of naturally occurring biotite and phlogopite. Two substitutions, $^{[6]}(Fe^{+2}Mg^{-1})$ and $^{[6,4]}(Al,Al)(Mg,Si)_{-1}$, represent the principal compositional variations of natural samples in metamorphic assemblages (Guidotti, 1984). The four corresponding end-members are phlogopite (Phl) $KMg_3(AlSi_3)O_{10}(OH)_2$, annite (Ann) $KFe_3(AlSi_3)O_{10}(OH)_2$, eastonite (East) $K(Mg_2Al)(Al_2Si_2)O_{10}(OH)_2$, and siderophyllite (Sdp) $K(Fe_2Al)(Al_2Si_2)O_{10}(OH)_2$.

The range of solid solution among these end-members and some properties of the solid solutions have been studied previously. The phlogopite-annite solid solution behaves approximately ideally, based on phase equilibria experiments (Wones and Eugster, 1965; Wones, 1972) and observations on Fe-Mg distributions in natural biotite (Mueller, 1972). Rutherford (1973) investigated the join annite-siderophyllite, determined an upper $^{[6,4]}$Al substitution limit of $Ann_{25}Sdp_{75}$, and concluded from phase equilibria experiments at $P_{fluid} = 2$ kbar that $^{[6,4]}$Al-rich annite is stable to higher temperatures than the end-member annite, eventually breaking down to sanidine + magnetite-hercynite solid solutions + corundum + leucite + vapor. Hewitt and Wones (1975) studied the effect of compositional variation on the unit-cell volume of synthetic iron magnesium aluminum biotite. They reported the same extent of $^{[6,4]}$Al substitution in annite as Rutherford (1973) and observed an upper $^{[6,4]}$Al substitution limit of $Phl_{38}East_{62}$ for the phlogopite-eastonite join. They proposed ideal solution behavior for the phlogopite-annite and phlogopite-eastonite solid solutions, based

* Present address: Department of Earth and Planetary Sciences, Harvard University, Cambridge, Massachusetts 02138, U.S.A.

0003–004X/92/1112–1191$02.00

on approximately linear decreases in unit-cell volume with increasing [6]Mg and [6,4]Al content, respectively. They concluded that the annite-siderophyllite join behaves nonideally, on the basis of the positive deviation of the unit-cell volume from ideal mixing. However, although a nonideal volume of mixing will change the activity-composition relations as a function of pressure, an ideal volume of mixing does not require the solid-solution behavior to be ideal. Other experimental data on the phlogopite-eastonite join (Robert, 1976) indicate that the upper limit of [6,4]Al substitution in synthetic phlogopite decreases with increasing temperature from $X_{East} \approx 0.5$ at 873 K to $X_{East} \approx 0.00$ at 1273 K (1.0 kbar), although at 1273 K, 5.0 kbar, Circone et al. (1991) observed limited solid solution (to $X_{East} \approx 0.38$) in their synthesis experiments. In natural samples, the observed range of solid solution is limited to $X_{East} < 0.50$ (Guidotti, 1984; Livi and Veblen, 1987).

This study focuses on the thermodynamic properties and solid-solution behavior of the phlogopite-eastonite join, determined from high-temperature lead borate solution calorimetry on a series of well-characterized synthetic magnesium aluminum phlogopite samples. Recently this technique has been successfully applied to hydrous phases such as talc, tremolite, brucite (Kiseleva and Ogorodova, 1984), phlogopite (and brucite again, Clemens et al., 1987), and tremolite-richterite solid solutions (A. Pawley, unpublished data). In this study, the heat capacities between 298 and 673 K and the enthalpies of solution at 977 K of magnesium aluminum phlogopite with varying [6,4]Al content are measured. The enthalpy of mixing is determined from the solution calorimetry data. Using these results and the calculated configurational entropy of the solid solution, we calculate the standard-state enthalpies (1 bar, 298.15 K) and Gibbs free energies of formation of phlogopite and eastonite. The activity-composition relations as a function of temperature have been computed. The thermodynamic data from this study are then used to calculate the equilibrium for the reaction

$$KMg_3(AlSi_3)O_{10}(OH)_2 + 3\ SiO_2 = KAlSi_3O_8 + 3\ MgSiO_3 + H_2O \qquad (1)$$

as a function of pressure, temperature, and the [6,4]Al content of phlogopite. Phase equilibria studies on the stability of phlogopite in the presence of quartz (e.g., Bohlen et al., 1983; Peterson and Newton, 1989; Montana and Brearley, 1989) have defined the phase relationships for this system, although the experimentally determined positions of the reactions exhibit some inconsistencies (Montana and Brearley, 1989). Reaction 1 is metastable over much of the pressure and temperature range of geologic interest because of the intersection of the reaction with the solidus to produce hydrous silicate melt. Phase equilibria experiments on Reaction 1 have been done at pressures ≤ 0.5 kbar (Peterson and Newton, 1989) or at higher pressure by adding CO_2 to reduce the activity of H_2O and inhibit melt formation (Bohlen et al., 1983). The position in P,T space of the equilibria that involve the formation of silicate melt (see Montana and Brearley, 1989, for a review of the phase relationships) cannot be calculated from thermodynamic data because the properties of the hydrous silicate melt are unknown. Thus, we have used Reaction 1, even though it represents a metastable equilibrium, to assess the thermodynamic data set obtained in this study.

Summary of sample synthesis and characterization

The synthetic magnesium aluminum phlogopite samples used in this study are the same materials used in a recent structural study (Circone et al., 1991), and the relevant data are summarized below. The samples were synthesized from gel starting materials at 673–923 K, 5.0 kbar. The synthetic mica compositions, determined by electron microprobe analysis, correspond to the chemical formula $K(Mg_{3-X}Al_X)(Al_{1+X}Si_{3-X})O_{10}(OH)_2$, with observed mole fractions of [6,4]Al substitution of $X_{East} \approx 0.00$, 0.13, 0.24 (0.3), 0.32 (1.4), 0.45 (1.7), 0.56 (1.7), 0.70 (1.8), 0.80 (2.6) and 0.92 (3.9), where the samples with $X_{East} \geq 0.24$ contain increasing amounts of excess α-Al_2O_3 (indicated in parentheses in weight percent). Although the compositions of the starting materials were stoichiometric, all of the synthetic mica compositions indicate that [6]Al is slightly greater than [4]Al in excess of the end-member ($AlSi_3$) composition (Circone et al., 1991). For the reactants and products to balance, excess Al_2O_3 and small amounts of K_2O and MgO must be present in the experiment products. The last two oxides remain in the excess fluid phase, whereas the Al_2O_3, which is more insoluble, remains in the charge; there is no excess SiO_2 phase. Thus, only a correction for excess Al_2O_3 is needed (see below).

The observed range of X_{East} substitution extends approximately to the eastonite end-member and is greater than that of $X_{East} \approx 0.62$ proposed by Hewitt and Wones (1975). The unit-cell volume of magnesium aluminum phlogopite, obtained from powder X-ray diffraction data, decreases linearly with increasing [6,4]Al content. This trend is identical to that observed by Hewitt and Wones (1975) and indicates that the volume of mixing is zero. Thermogravimetric analyses of the synthetic micas from 303 to 1403 K indicate that: (1) samples with $0.00 \leq X_{East} \leq 0.45$ lose a minor amount of weight (~0.4 wt%) between 303 and ~1003 K because of adsorbed H_2O loss and (2) samples with $X_{East} \geq 0.56$ lose ~1.8% of their weight between 303 and 1003 K because of adsorbed H_2O loss and partial dehydroxylation of the mica above 723 K. These results are considered below in the measurement of the heat capacities between 298 and 673 K and the enthalpies of solution at 977 K.

Analysis and computer modeling of ^{29}Si MAS NMR spectra of the synthetic magnesium aluminum phlogopite samples indicate that the Al,Si distribution in the tetrahedral sites is primarily constrained by the avoidance of adjacent Al tetrahedra (Circone et al., 1991). The tetra-

hedral sheet compositions of the samples, calculated assuming that adjacent Al tetrahedra are not present, closely agree with those measured by electron microprobe analysis. The avoidance of [4]Al-O-[4]Al linkages is observed for a variety of micas and clays of natural (e.g., Sanz and Serratosa, 1984; Herrero et al., 1985a) and synthetic (e.g., Herrero et al., 1985b, 1987) origin. Comparison of computer-simulated Al,Si distributions with those inferred from the ^{29}Si NMR spectra exclude both a random distribution and a long-range ordered distribution. Instead, the Al,Si distribution lies somewhere between these two extremes and is constrained primarily by the avoidance of [4]Al-O-[4]Al linkages. As the [4]Al/[4](Al + Si) ratio approaches 0.5, the Al,Si distribution in magnesium aluminum phlogopite becomes increasingly ordered and converges with the long-range ordered distribution.

Calorimetric techniques

Differential scanning calorimetry

The high-temperature heat capacities of the synthetic magnesium aluminum phlogopite samples with X_{East} = 0.00, 0.24, and 0.45 were measured with a Setaram DSC-111 differential scanning calorimeter. Samples weighing 95–100 mg were packed into cylindrical Pt pans with Pt lids. Samples were heated overnight at 373 K in Ar gas in the calorimeter to drive off adsorbed H_2O. Heat capacities were measured between 298 and 673 K using a step scan routine, which involved heating at 2 K/min for 5 min, followed by isothermal equilibration for 5 min. Sample weights measured before and after the heat-capacity measurements indicated that the samples had not decomposed during the experiments. The averaged data from three scans were analyzed in the following way. Four identical scans on α-Al_2O_3 powder were averaged and used to calibrate the heat-capacity data. Four averaged blank experiments (empty pans with lids) were subtracted from the mica and α-Al_2O_3 experiments to correct for baseline effects from the instrument. The accuracy of the procedure for measuring heat capacities was confirmed by measuring the heat capacity of silica glass, in which the results of Richet et al. (1982) were reproduced within 1% between 298 and 673 K. The measured heat capacities for the samples with X_{East} = 0.24 and 0.45 are corrected for excess corundum (using the heat capacity for α-Al_2O_3 from Robie et al., 1978; the correction is $\ll$0.5% of C_P). The errors in our measurements are estimated to be $\pm$1.5%.

High-temperature solution calorimetry

A Calvet-type twin calorimeter operating at 977 K was used to measure the enthalpy of solution of the magnesium aluminum phlogopite samples in molten lead borate solvent ($2PbO$-B_2O_3). The equipment and methods of data acquisition are described in detail in Navrotsky (1977). Three types of calorimetric experiments, all under static air atmosphere (see Appendix 1), were performed: solution calorimetry, drop solution calorimetry, and transposed temperature drop calorimetry. The sample weights in all experiments varied from 6 to 28 mg.

The solution calorimetry technique was used to measure the enthalpy of solution (ΔH_{soln}) of samples with $0.00 \leq X_{East} \leq 0.45$. The sample was weighed into Pt holders with perforated Pt foil bottoms, equilibrated for several hours in the calorimeter at 977 K, then stirred into 30 g of molten lead borate until completely dissolved. The stability of each mica under calorimeter conditions was confirmed by checking thermally equilibrated samples for weight loss and by powder X-ray diffraction.

A two-step cycle involving drop solution and transposed temperature drop calorimetry was used to measure the ΔH_{soln} of the synthetic magnesium aluminum phlogopite samples with $0.56 \leq X_{East} \leq 0.92$, since solution calorimetry requires several hours of equilibration at ~973 K, and these samples lost weight irreversibly between 723 and 1003 K in the thermogravimetric experiments. In the drop solution experiments, the sample was weighed into capsules of lead borate glass (made by dipping a tapered graphite rod into molten lead borate, quenching the capsule on the rod, sliding it off, then annealing it at 573 K for a minimum of 24 h). The sample and capsule were equilibrated at room temperature, then dropped into the calorimeter and molten lead borate. The measured heat effect was corrected for the enthalpy of the capsule, which was determined from several drop solution experiments on empty capsules. The remainder is the enthalpy of drop solution (ΔH_{dsoln}), which contains the heat content H^0_{977}-H^0_{298} plus the ΔH_{soln} of the mica. Since the heat capacities of these samples were not measured, their heat contents were determined by dropping samples in crimped-shut Pt foil capsules into the calorimeter in the absence of molten lead borate. The measured heat effect ΔH_{drop}, corrected for the heat content of the Pt foil capsule, was subtracted from ΔH_{dsoln} to obtain ΔH_{soln} in molten lead borate at 977 K. The measured weight losses of the samples used in the heat-content measurements suggest that insignificant weight loss due to mica dehydroxylation occurred during these measurements. The samples lost ~1.8 wt% between 303 and 1003 K in the thermogravimetric analysis experiments, primarily from the loss of adsorbed H_2O (Circone et al., 1991). Samples dropped in the heat-content measurements (298–977 K) lost only 1.2 $\pm$ 0.2 wt% (based on 14 measurements), and this weight loss is wholly attributable to the loss of adsorbed H_2O based on the thermogravimetric results and expected mica H_2O contents.

The data for the samples containing excess Al_2O_3 were corrected using the heat content (ΔH_{drop} = 75.2 $\pm$ 0.8 kJ/mol; Robie et al., 1978) and the enthalpy of solution (ΔH_{soln} = 32.8 $\pm$ 0.3 kJ/mol; Navrotsky et al., 1986) of α-Al_2O_3. For the samples with X_{East} = 0.24, 0.32, and 0.45, the corrections to the enthalpies of solution are 0.1, 0.7, and 0.8%, respectively, of the measured enthalpies in joules. The corrections to the heat content are 1.5, 1.7, 2.4, and 3.6%, and the corrections to the enthalpies of

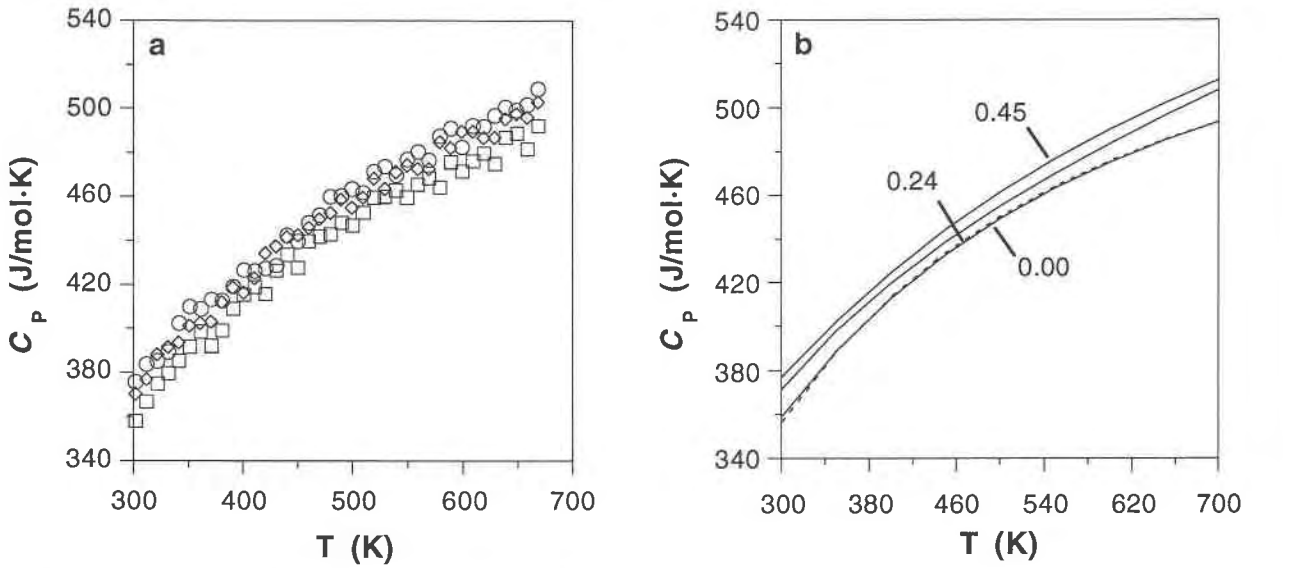

Fig. 1. (**a**) Measured heat capacity data of the magnesium aluminum phlogopite samples with X_{East} = 0.00 (squares), 0.24 (diamonds), and 0.45 (circles). Systematic deviations in the data arise from subtracted blank and α-Al_2O_3 calibration scans. (**b**) Heat capacity curves (labeled by X_{East} content) calculated from least-squares polynomial fits (Table 1) based on the data shown in **a**. The heat capacity of a natural phlogopite sample (Robie and Hemingway, 1984) is shown for comparison (dashed curve).

drop solution are 1.3, 1.3, 1.8, and 2.8% of the measured enthalpies in joules for the samples with X_{East} = 0.56, 0.70, 0.80, and 0.92, respectively.

The drop solution cycle was checked by measuring ΔH_{dsoln} of α-Al_2O_3. The measured ΔH_{dsoln} (ΔH_{dsoln} = 108.6 ± 1.9 kJ/mol, based on 14 experiments) is identical within experimental error to the sum of the ΔH_{soln} (Navrotsky et al., 1986) plus the heat content (Robie et al., 1978) of α-Al_2O_3. Further checks on the validity of the calorimetric techniques for hydrous phases are discussed in Appendix 1.

Heat capacity between 298 and 673 K, X_{East} = 0.00, 0.24, and 0.45

Results

The heat-capacity data (Fig. 1a) were fitted by least squares to the equation $C_P = a + bT + cT^{-2} + dT^{-0.5}$ (Table 1, Fig. 1b). The coefficients are based on the molecular weight calculated from the electron microprobe analyses (Table 2 in Circone et al., 1991) and are not corrected for the effects of small deviations from the ideal formulae. The measured C_P of the synthetic phlogopite (X_{East} = 0.00) in this study is within 1% of the heat capacity of a natural phlogopite sample measured by Robie and Hemingway (1984) (Fig. 1b). We have used their equation for the heat capacity of phlogopite for the calculations in this study because they measured heat capacity up to 1000 K and corrected for deviations from ideal composition. The measured C_P of the magnesium aluminum phlogopite samples appear to increase slightly with increasing [6,4]Al content, although the scatter in the data is comparable in magnitude to the increase in C_P (Fig. 1a). The C_P of the mica with X_{East} = 0.24 is ~2% higher, and the C_P of the mica with X_{East} = 0.45 is ~3% higher than the C_P of the phlogopite end-member (Fig. 1b).

Discussion

The heat capacities of the Al-rich synthetic samples were not measured because of possible decomposition during differential scanning calorimetry, in which each scan lasts over 6 h, and because sample quantities were limited. The heat capacity of eastonite can be estimated using the models of Robinson and Haas (1983) and Berman and Brown (1985), and their accuracy can be assessed by comparing the estimated C_P to the measured C_P of the three samples in this study. The results of both

Table 1. Coefficients for the heat capacity equations for three synthetic magnesium aluminum phlogopite samples

X_{East}	a	b	c	d	R^2
0.00	9.0885E + 2	−8.5874E − 2	2.2825E + 6	−9.5203E + 3	0.9959
0.24	9.6353E + 2	−8.8474E − 2	4.9178E + 6	−1.0744E + 4	0.9967
0.45	9.1529E + 2	−4.1859E − 2	5.5919E + 6	−1.0183E + 4	0.9958

Note: Measured heat capacities (in J/mol·K) are fit to the equation $C_P = a + bT + cT^{-2} + dT^{-0.5}$. Equations are valid from 298 to 673 K.

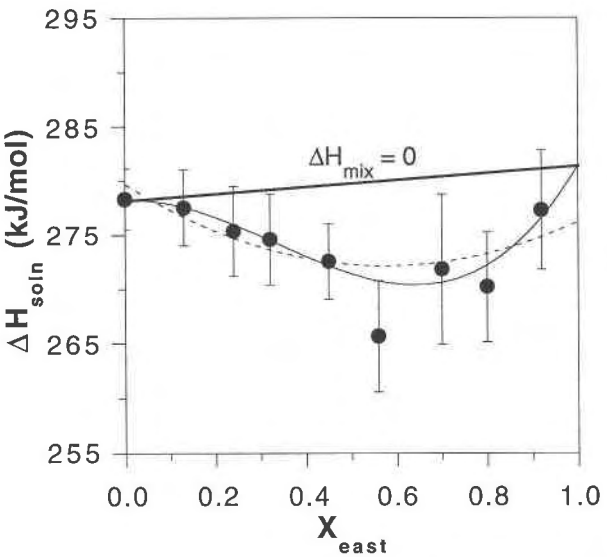

Fig. 2. Measured enthalpies of solution of the synthetic magnesium aluminum phlogopite samples. Brackets represent 2 sd of the mean. The dashed curve is the second-order polynomial least squares fit, and the solid curve is the third-order polynomial least squares fit through the sample means of the enthalpy of solution data. The solid line represents the ideal mixing line extrapolated to the estimated ΔH_{soln} of eastonite using the third-order polynomial (see text).

models are similar, and we will use the model of Berman and Brown (1985) for further discussion.

The estimated C_P of phlogopite is slightly higher but remains within 2.1% of the measured C_P (Robie and Hemingway, 1984; this study), which corresponds to an overestimation in the heat content H^0_{977}-H^0_{298} of +1.1%. However, the C_P models do not predict the observed increase in C_P with increasing [6,4]Al content. For the mica with $X_{East} = 0.24$, the model underestimates C_P by −1.5% at 673 K and −5.7% at 977 K, corresponding to underestimations in the heat content of −1.3% for H^0_{673}-H^0_{298} and of −2.4% for H^0_{977}-H^0_{298}. For the mica with X_{East} = 0.45, the model underestimates C_P by −2.3% at 673 K and by −3.6% at 977 K, corresponding to underestimations in heat content of −2.4% for H^0_{673}-H^0_{298} and of −2.7% for H^0_{977}-H^0_{298}.

If this trend continues for the micas with higher [6,4]Al contents, then the discrepancies between estimated and measured heat capacities and heat contents will increase. The heat content H^0_{977}-H^0_{298} of the micas with $0.70 \le X_{East} \le 0.92$, measured by transposed temperature drop calorimetry, is 334.81 ± 2.81 kJ/mol (note: the data for X_{East} = 0.56 have been omitted, see below). This value is based on the average of 14 drop experiments on the three samples because there is no discernible correlation between the measured heat contents and [6,4]Al content over this composition range. The estimated heat content with the model of Berman and Brown (1985) is 324.0 kJ/mol, which underestimates the measured heat content by −3.2% and is consistent with the trend described above.

Table 2. Enthalpies of solution and drop solution of synthetic magnesium aluminum phlogopite samples at 977 K in molten $2PbO\text{-}B_2O_3$

X_{East}	No. of experiments	ΔH_{dsoln}* (kJ/mol)	ΔH_{soln}* (kJ/mol)
0.00	9		278.37(2.78)
0.13	9		277.57(3.52)
0.24	9		275.36(4.18)
0.32	8		274.62(4.22)
0.45	8		272.58(3.52)
0.56	7	601.24(4.33)	266.43(5.16)**
0.70	8	606.67(6.35)	271.86(6.94)**
0.80	7	605.03(4.22)	270.22(5.07)**
0.92	7	612.14(4.75)	277.33(5.52)**

Note: Data corrected for excess α-Al_2O_3 in the samples with $0.24 \le X_{East} \le 0.92$.

* Numbers quoted are the mean of n experiments. Numbers in parentheses are 2 sd of the mean = $2sn^{-0.5}$, where s is the standard deviation of n experiments. The mean ± $2sn^{-0.5}$ represents a 95% confidence interval for the enthalpy of solution or drop solution.

** The $\Delta H_{soln} = \Delta H_{dsoln} - \Delta H_{drop}$, where ΔH_{drop} = 334.81(2.81) kJ/mol, the mean of 14 transposed temperature drop experiments on the samples with $0.70 \le X_{East} \le 0.92$.

However, since one heat-content measurement does not contain sufficient information for calculating dehydration equilibria, we will use the model of Berman and Brown (1985), which consistently underestimates the heat capacities of the magnesium aluminum phlogopite samples, and assess how the results change if the heat capacity of eastonite is higher.

Enthalpies of solution

Results

The measured enthalpies of solution and drop solution for the synthetic micas and the variation of ΔH_{soln} with [6,4]Al content (Table 2, Fig. 2) suggest a large, positive asymmetric deviation from ideal mixing. We have excluded the data for X_{East} = 0.56 from our analysis of the enthalpy of solution data because the data deviate significantly from the trend defined by the entire data set, the X-ray diffraction data indicate that the sample is poorly crystallized, and its unit-cell volume deviates significantly from the ideal volume of mixing trend (Circone et al., 1991).

The simplest mixing model is the regular solution model, defined as

$$\Delta H_{mix} = W^H X_{East}(1 - X_{East}) \quad (2)$$

where W^H is the enthalpic interaction parameter. The least squares fit through the sample means of the ΔH_{soln} data ($\Delta H_{soln} = 279.73 - 26.30X_{East} + 22.81X^2_{East}$, Fig. 2) yields W^H = 22.8 ± 18.7 kJ/mol, extrapolates to a ΔH_{soln} of eastonite of 276.0 ± 5.7 kJ/mol, accounts for only 68% of the observed variation in ΔH_{soln}, and does not account for the apparent asymmetry of the data, although a second-order polynomial fit does pass through the ranges defined by the uncertainties in the sample means (Fig. 2).

The subregular solution model is the simplest asymmetric nonideal solution model, and the enthalpy of mixing is defined as

$$\Delta H_{mix} = W^H_{East} X_{East}(1 - X_{East})^2 + W^H_{Phl} X^2_{East}(1 - X_{East}) = W^H_{East} X_{East} + (W^H_{Phl} - 2W^H_{East}) X^2_{East} + (W^H_{East} - W^H_{Phl}) X^3_{East} \quad (3)$$

where W^H_{East} and W^H_{Phl} are the excess mixing parameters. The least-squares polynomial fit to the ΔH_{soln} data ($\Delta H_{soln} = 278.20 + 2.71X_{East} - 65.42X^2_{East} + 65.86X^3_{East}$) yields $W^H_{Phl} = 66.3 \pm 17.3$ kJ/mol, $W^H_{East} = 0.4 \pm 43.2$ kJ/mol, extrapolates to a ΔH_{soln} of eastonite of 281.4 ± 2.6 kJ/mol, and accounts for 89% of the observed variation in ΔH_{soln}. The uncertainties for these values, calculated from the standard error estimates of the polynomial coefficients (W^H_{East} and W^H_{Phl}) or of the enthalpy of solution ($\Delta H_{soln,East}$), represent a 95% confidence interval.

Discussion

Ideally, one would like to fit the enthalpy of solution data with the simplest equation, i.e., the simplest mixing model, to describe the variation with composition (e.g., Navrotsky, 1987). This suggests that the second-order polynomial (regular solution model), which does not provide the best fit through the mean value for each sample but lies within the uncertainties denoted by the brackets in Figure 2, may be the preferred fit. However, this analysis of the data ignores what is known about the effect of the [6,4](Al,Al)(Mg,Si)$_{-1}$ substitution on the phlogopite crystal structure and the substitution limits implied by natural trioctahedral mica compositions.

The most significant factor affecting the range and stability of a solid solution is the strain energy associated with the size difference between the species that are mixing (Navrotsky, 1987). The large, endothermic enthalpy of mixing for the phlogopite-eastonite join suggests a tendency toward exsolution. The apparent asymmetry of the enthalpy of mixing and the relationship $W^H_{Ph} \gg W^H_{East}$ suggest that the solid solution is destabilized more by the substitution of [6]Mg,[4]Si into eastonite than by substitution of [6]Al,[4]Al into phlogopite. The estimated unit-cell volume of the eastonite end-member is 1.5% smaller than that of phlogopite. Although the difference in volume is not large, the effect of increasing [6,4]Al content on the mica structure is significant. As discussed in Hewitt and Wones (1975) and Circone et al. (1991), the [6,4]Al substitution in phlogopite increases the lateral misfit between the smaller octahedral and the larger tetrahedral sheets. The structure partially compensates for the misfit by increasing the counterrotation of contiguous tetrahedra in the basal plane (tetrahedral rotation). The maximum amount of tetrahedral rotation, which reduces the size of the interlayer site, is ultimately limited by the size of the interlayer cation and is approached as the [6,4]Al content of magnesium aluminum phlogopite increases to $X_{East} = 1.00$. Thus, substituting the larger phlogopite constituent into the smaller, strained eastonite structure is energetically costly, and this is consistent with a large, asymmetric, and endothermic enthalpy of mixing for the join. Furthermore, in natural samples the extent of [6,4](Al,Al)(Mg,Si)$_{-1}$ substitution is limited to $X_{East} < 0.50$, and the Al-rich compositions have not been observed, again suggesting that the solid-solution properties of the join are not symmetrically related. This is discussed in greater detail below.

Enthalpies of formation

The standard-state enthalpies of formation from the elements ($\Delta H^0_{f,298}$) of phlogopite and eastonite can be calculated from the following thermodynamic data: enthalpies of solution of the micas and of their constituent oxides near 973 K, heat capacities of the micas and the oxides, and enthalpies of formation from the elements of the oxides (Table 3). The heat content of $Mg(OH)_2$ is extrapolated 77 K above the valid temperature range (298–900 K) in Robie et al. (1978), but the uncertainty from the extrapolation is small because heat capacity varies slowly at high temperature.

The enthalpy of formation of phlogopite has been calculated using the reaction

$$KAlSi_3O_8 + 2MgO + Mg(OH)_2 = KMg_3(AlSi_3)O_{10}(OH)_2. \quad (4)$$

The enthalpy of formation from the oxides at 977 K is calculated using $\Delta H_{f,Ox,977} = \Sigma\, \Delta H_{soln,react} - \Sigma\, \Delta H_{soln,prod} = -126.3 \pm 3.6$ kJ/mol. Then $\Delta H_{f,Ox,977}$ is corrected to 298 K using $\Delta H_{f,Ox,298} = \Sigma\, (H_{298}\text{-}H_{977})_{react} - \Sigma\, (H_{298}\text{-}H_{977})_{prod} = -124.6 \pm 4.5$ kJ/mol. Adding the enthalpies of formation from the elements of the oxides in Reaction 4, we obtain $\Delta H^0_{f,298} = -6211.7 \pm 5.6$ kJ/mol. Clemens et al. (1987) obtained $\Delta H^0_{f,298} = -6214.1 \pm 6.1$ kJ/mol using their measured $\Delta H_{soln,Phl}$ of 281.9 ± 5.1 kJ/mol and the $\Delta H^0_{f,298}$ of brucite from Robie et al. (1978).

Similarly, the enthalpy of formation from the elements of eastonite has been calculated using the reaction

$$KAlSi_3O_8 + MgO + Mg(OH)_2 + Al_2O_3 = K(Mg_2Al)(Al_2Si_2)O_{10}(OH)_2 + SiO_2. \quad (5)$$

On the basis of the same cycle described above, $\Delta H_{f,Ox,977} = -97.8 \pm 3.4$ kJ/mol. If the estimated heat capacity from Berman and Brown (1985) is used, then $\Delta H_{f,Ox,298} = -101.6 \pm 7.5$ kJ/mol and $\Delta H^0_{f,298} = -6352.2 \pm 8.4$ kJ/mol. If the heat content measured by transposed temperature drop calorimetry is used for the correction to 298 K, then $\Delta H_{f,Ox,298} = -112.4 \pm 4.7$ kJ/mol and $\Delta H^0_{f,298} = -6363.0 \pm 6.0$ kJ/mol. These $\Delta H^0_{f,298}$ are 16–26 kJ/mol more exothermic than that of -6336.6 ± 3.8 kJ/mol, estimated by Holland and Powell (1990). The values for $\Delta H^0_{f,298}$ of eastonite will be compared in the calculation of P,T equilibria of magnesium aluminum phlogopite.

Vibrational and configurational entropies

Vibrational entropies

The measured vibrational entropy of phlogopite at 1 bar, 298 K (S^0_{298}) is 315.9 ± 1.0 J/mol·K (Robie and

TABLE 3. Thermodynamic data (in kJ/mol) used to calculate $\Delta H^0_{f,298}$ of phlogopite and eastonite

Compound	$\Delta H_{soln,\sim 977}$	$H^0_{977}-H^0_{298}$ [A]	$\Delta H^0_{f,298}$
$KAlSi_3O_8$	94.43(138)[B]	186.95(131)	−3959.56(337)
MgO	4.88(62)[C]	31.81(23)	−601.49(29)
$Mg(OH)_2$	47.92(162)[D]	69.84(49)	−924.54(44)
Al_2O_3	32.77(33)[E]	75.07(52)	−1675.70(130)
SiO_2	−3.51(17)[F]	43.47(30)	−910.70(100)
$KMg_3(AlSi_3)O_{10}(OH)_2$	278.37(278)[G]	318.80(223)[H]	−6211.73(564)[G]
		318.71(478)[I]	
$K(Mg_2Al)(Al_2Si_2)O_{10}(OH)_2$	281.35(259)[G]	334.81(281)[G]	−6363.04(602)[G]
		324.00(648)[J]	−6352.23(839)[G]

Note: Data from Robie et al. (1978), except where noted. Numbers in parentheses are uncertainties in the last significant figures.
[A] Uncertainties are estimated to be ±0.7% of the heat content quoted, except where noted.
[B] Clemens et al. (1987) and references therein.
[C] Davies and Navrotsky (1981).
[D] The $\Delta H_{soln} = \Delta H_{dsoln} - (H^0_{977}-H^0_{298})$, where ΔH_{dsoln} = 117.76(1.54) kJ/mol (S. Circone, unpublished data).
[E] Navrotsky et al. (1986).
[F] Akaogi and Navrotsky (1984).
[G] This study.
[H] Robie and Hemingway (1984).
[I] This study, uncertainty is ±1.5%.
[J] Estimated using the model of Berman and Brown (1985), uncertainty is ±2%.

Hemingway, 1984) (Table 4). The vibrational entropy of eastonite can be estimated using the exchange reaction

$$K(Mg_2Al)(Al_2Si_2)O_{10}(OH)_2 + MgO + SiO_2 = KMg_3(AlSi_3)O_{10}(OH)_2 + Al_2O_3 \quad (6)$$

and the empirical algorithm of Helgeson et al. (1978, Eq. 62):

$$S^0_{mica} = S^0_r (V^0_r + V^0_{mica})(2V^0_r)^{-1} \quad (7)$$

where

$$S^0_r = S^0_{Phl} + X_{East}(S^0_{Al_2O_3} - S^0_{MgO} - S^0_{SiO_2}) \quad (8)$$

and

$$V^0_r = V^0_{Phl} + X_{East}(V^0_{Al_2O_3} - V^0_{MgO} - V^0_{SiO_2}). \quad (9)$$

Similarly, exchange reactions involving isostructural end-member pairs such as akermanite ($Ca_2MgSi_2O_7$), gehlenite ($Ca_2Al_2SiO_7$), diopside ($CaMgSi_2O_6$), and aluminum pyroxene ($CaAl_2SiO_6$) can be used in place of the simple oxides in Reaction 6. The entropy and volume data used to calculate the vibrational entropy of eastonite are in Table 4. The molar volume of eastonite was extrapolated from the linear regression of the unit-cell volume data of the synthetic magnesium aluminum phlogopite samples (Table 4 in Circone et al., 1991), excluding the data for the sample with $X_{East} = 0.56$. Since corundum (all [6]Al) is used in the exchange reaction involving simple oxides, and half of the added Al in eastonite is tetrahedrally coordinated, the calculated vibrational entropy of eastonite must be corrected for the Al coordination change. The entropy change was estimated from the kyanite-sillimanite transition (all [6]Al for kyanite, ½[6]Al, ½[4]Al for sillimanite) where $\Delta S^0_{298} = 12.4 \pm 0.5$ J/mol·K. With Reaction 6, the calculated vibrational entropy of magnesium aluminum phlogopite increases slightly with increasing [6,4]Al content to 317.4 ± 1.2 J/mol·K for the eastonite end-member (Table 4, Fig. 3). For the exchange reaction involving akermanite-gehlenite, the calculated vibrational entropy of eastonite is 316.67 ± 2.85 J/mol·K, identical to the results obtained using the simple oxides. The anomalous value of 329.15 ± 4.22 J/mol·K obtained using an exchange reaction with diopside–aluminum pyroxene probably arises from a configurational entropy term included in the tabulated value for aluminum pyroxene (Robie et al., 1978). Since the configurational model used is not defined and the extent of short-range ordering in aluminum pyroxene is not well known, we do not consider this result to be as reliable as the others. We have used the results obtained with Reaction 6 in all calculations. The S^0_{298} for phlogopite estimated using this algorithm (318.4 J/mol·K; Helgeson et al., 1978) is within 1% of the measured value, but it may be less reliable for magnesium aluminum phlogopite because distortions

TABLE 4. Standard-state molar volumes and entropies of minerals used to calculate the vibrational entropy of $K(Mg_2Al)(Al_2Si_2)O_{10}(OH)_2$

Compound	S^0_{298} (J/mol·K)	V^0_{298} (J/bar)
Al_2O_3	50.92(10)	2.5575(7)
MgO	26.94(17)	1.1248(4)
SiO_2	41.46(20)	2.2688(1)
$Ca_2Al_2SiO_7$	209.80(164)	9.024(9)
$Ca_2MgSi_2O_7$	209.33(209)	9.281(9)
$CaAl_2SiO_6$	156.00(400)	6.350(9)
$CaMgSi_2O_6$	143.09(84)	6.609(10)
$KMg_3(AlSi_3)O_{10}(OH)_2$	315.90(100)*	14.9674(33)**
$K(Mg_2Al)(Al_2Si_2)O_{10}(OH)_2$	317.45(120)†	14.7385(94)**
	316.67(285)‡	
	329.15(422)§	

Note: Data from Robie et al. (1978), except where noted. Numbers in parentheses are uncertainties in the last significant figures.
* Robie and Hemingway (1984); excludes configurational entropy contribution.
** Circone et al. (1991).
† This study, using exchange reaction with simple oxides.
‡ This study, using exchange reaction with gehlenite and akermanite.
§ This study, using exchange reaction with diopside and Al pyroxene.

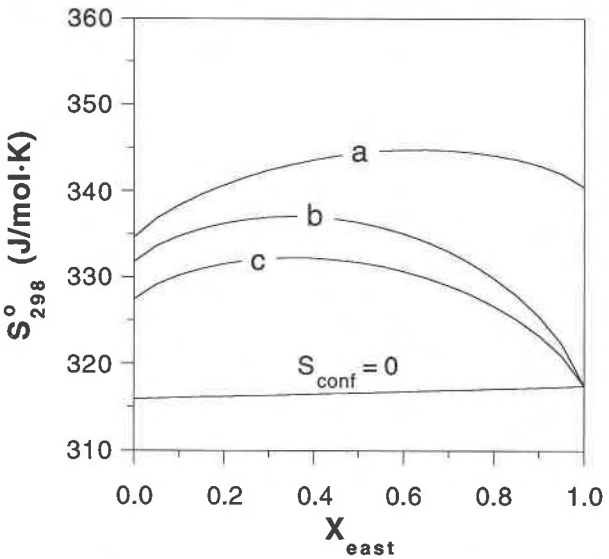

Fig. 3. Calculated entropies of micas on the phlogopite-eastonite join. Curves a, b, and c include the configurational entropy arising from Mg,Al mixing on one M site plus the configurational entropy arising from Al,Si mixing on the T sites with a random (a), short-range ordered (b), or long-range ordered (c) Al,Si distribution.

in the octahedral and tetrahedral sites in the micas would not be represented accurately by the analogues used in the exchange reactions.

Configurational entropies

Mixing of Mg and Al on octahedral sites (M) and mixing of Al and Si on tetrahedral sites (T) contribute to the entropy of magnesium aluminum phlogopite. The configurational entropy arises from the number of spatial configurations available to a system containing a mixture of N_A A atoms and N_B B atoms on a structural site and is defined as

$$S_{conf} = k \ln \Omega = k \ln \frac{(N_A + N_B)!}{N_A! N_B!} \quad (10)$$

where k is Boltzmann's constant and Ω is the number of permutations of $N_A + N_B$ atoms, excluding the indistinguishable permutations in which like atoms are interchanged. When the atoms mix randomly on the sites, Equation 10 can be generalized and rewritten, using Stirling's approximation, as:

$$S_{conf} = -R \sum_j n_j (X_j^k \ln X_j^k) \quad (11)$$

where R is the gas constant, n_j is the number of moles of structural site j per formula unit, and X_j^k is the mole fraction of atom k on site j.

Mixing on M sites. The [6]Mg and [6]Al cations can potentially mix on three octahedral sites. On the basis of structure refinements of natural trioctahedral micas, the M1 site, with OH anions in opposite corners of the octahedral site, is on average larger than the M2 sites, which are approximately equal in size and have OH anions located on adjacent corners of the octahedral sites. Three Mg,Al mixing models are possible: (1) mixing occurs on all three M sites, (2) mixing is limited to the two M2 sites, or (3) mixing is limited to the M1 site. The latter two distributions have been observed for two samples of natural clintonite, a trioctahedral brittle mica with the same octahedral composition as eastonite (Guggenheim, 1984, and references therein). Although we would expect that the smaller, higher charge Al cation would be ordered on the smaller M2 sites (Bailey, 1984), IR and Raman spectra of the magnesium aluminum phlogopite samples in this study suggest that Al is ordered on a single octahedral site. We observe only two bands in the −OH stretching region (S. Circone, unpublished data) that correspond to −OH adjacent to $3Mg^{2+}$ and to $2Mg^{2+}Al^{3+}$ (Vedder and Wilkins, 1969). If Mg,Al are randomly distributed on the M2 sites, a third band corresponding to −OH adjacent to $Mg^{2+}2Al^{3+}$ would be present. Therefore, we have adopted a one-site mixing model for the configurational entropy of the M sites, where

$$S^M_{conf} = -R(X^{Al}_M \ln X^{Al}_M + X^{Mg}_M \ln X^{Mg}_M). \quad (12)$$

This expression can be rewritten in terms of X_{East} by substituting $X^{Al}_M = X_{East}$ and $X^{Mg}_M = (1 - X_{East})$ into Equation 12. The configurational entropy of the M sites becomes

$$S^M_{conf} = -R[X_{East} \ln X_{East} + (1 - X_{East}) \ln (1 - X_{East})]. \quad (13)$$

Mixing on T sites. The results of ^{29}Si NMR for the magnesium aluminum phlogopite samples suggest that [4]Al-O-[4]Al linkages are not present in the tetrahedral sheets, consistent with several studies of ^{29}Si MAS NMR on trioctahedral clays and micas with [4]Al/[4](Al + Si) ratios between 0.0 and 0.5. Thus, the random four-site mixing model, where $S^{T,ran}_{conf} = -4R(X^{Al}_T \ln X^{Al}_T + X^{Si}_T \ln X^{Si}_T)$, used by Bohlen et al. (1983) and Clemens et al. (1987) in the calculation of phlogopite equilibria, is not the best model for the T-site configurational entropy. An alternative model that is consistent with [4]Al-O-[4]Al avoidance is the long-range ordered distribution, where Al and Si mix randomly on one set of tetrahedral sites (T1) that alternate with Si-only tetrahedral sites (T2). The configurational entropy of an ordered Al,Si distribution is $S^{T,ord}_{conf} = -2R(X^{Al}_{T1} \ln X^{Al}_{T1} + X^{Si}_{T1} \ln X^{Si}_{T1})$, and $S_{conf} = 0$ for the T2 sites. Computer simulations of the NMR spectra suggest that the ordered model also does not represent the distribution of Al and Si in the tetrahedral sites accurately, but it is significantly better than the random distribution model at high [4]Al contents (Circone et al., 1991). X-ray diffraction studies of 1M phlogopite and biotite also indicate that long-range Al,Si ordering is not common in natural 2:1 layer silicates (Bailey, 1984). Instead, the Al,Si distribution is short-range ordered, constrained mainly by the avoidance of contiguous Al tetrahedra. The configurational entropy must lie somewhere between the two extremes of complete randomness and complete or-

der, and as the $^{[4]}Al/^{[4]}(Al + Si)$ ratio approaches 0.5 (i.e., the eastonite end-member), the Al,Si distribution converges with the long-range ordered distribution.

A short-range ordered Al,Si distribution has been approximated using a one-dimensional array of tetrahedra analogous to a pyroxene chain. This model imposes an upper limit on the configurational entropy of the T sites. The expression for the configurational entropy of this linear model is

$$S_{\text{conf}}^{\text{T,lin}} = -\text{R}\left[(3 - X_{\text{East}})\ln\frac{2(1 - X_{\text{East}})}{(3 - X_{\text{East}})} - (1 + X_{\text{East}})\ln\frac{2(1 - X_{\text{East}})}{(1 + X_{\text{East}})}\right] \quad (14)$$

and is derived in Appendix 2. This linear model has been adopted in all of the calculations for activity-composition relations and phlogopite equilibria that follow. The random and ordered T-site models will be considered and their effect on the calculated activities and P,T positions of phlogopite equilibria will be addressed.

The calculated entropy of magnesium aluminum phlogopite is $S^{\circ}_{298,\text{ss}} = S^{\circ}_{298} + S^{\text{M}}_{\text{conf}} + S^{\text{T,lin}}_{\text{conf}}$ (Fig. 3). The phlogopite end-member, with the contribution of 15.9 J/mol·K from Al,Si mixing on T sites, has a standard-state entropy of 331.8 ± 1.0 J/mol·K. The eastonite end-member, which has no configurational contribution to its entropy because the M and T sites are fully ordered, has a standard-state entropy of 317.4 ± 1.2 J/mol·K. Since the eastonite-rich solid solutions decompose at high temperatures, a complete set of heat capacities from 298 to 1200 K cannot be measured. Furthermore, low-temperature heat capacities have not been measured for the solid-solution series, and such measurements are unlikely to be made because several grams of sample are required. Without this information we cannot completely rule out an excess vibrational contribution to the heat capacities and to the entropy of mixing. However, IR and Raman spectra of the magnesium aluminum phlogopite samples show no anomalies (S. Circone, unpublished data), and the assumption of zero excess vibrational contributions appears to be reasonable.

Gibbs free energies of formation

The standard entropies of formation from the elements ($\Delta S^{\circ}_{\text{f},298}$) of phlogopite and eastonite can be calculated using the tabulated S°_{298} data for the elements of Robie et al. (1978), the measured S°_{298} of phlogopite, and the calculated S°_{298} of eastonite (Table 4). The calculated entropy of formation of phlogopite, which includes the T-site configurational entropy calculated from Equation 14, is $\Delta S^{\circ}_{\text{f},298} = -1277.3 \pm 1.1$ J/mol·K. With the relationship $\Delta G^{\circ}_{\text{f},298} = \Delta H^{\circ}_{\text{f},298} - \text{T}\Delta S^{\circ}_{\text{f},298}$ and the $\Delta H^{\circ}_{\text{f},298}$ from this study (Table 3), the Gibbs free energy of formation of phlogopite is $\Delta G^{\circ}_{\text{f},298} = -5830.9 \pm 5.7$ kJ/mol. This value is slightly less exothermic than the $\Delta G^{\circ}_{\text{f},298} = -5834.1 \pm 6.3$ kJ/mol calculated from the results of Clemens et al. (1987), who obtained a slightly more exothermic $\Delta H^{\circ}_{\text{f},298}$ and assumed a random mixing model for the T sites, but the two values are within the uncertainties quoted.

The calculated entropy of formation of eastonite is $\Delta S^{\circ}_{\text{f},298} = -1296.8 \pm 1.2$ J/mol·K. If the $\Delta H^{\circ}_{\text{f},298}$ calculated using the estimated heat capacity of Berman and Brown (1985) is used (−6352.2 ± 8.4 kJ/mol, Table 3), then $\Delta G^{\circ}_{\text{f},298} = -5965.6 \pm 8.4$ kJ/mol. If the $\Delta H^{\circ}_{\text{f},298}$ calculated using the measured heat content of the Al-rich phlogopite samples is used (−6363.0 ± 6.0 kJ/mol, Table 3), then $\Delta G^{\circ}_{\text{f},298} = -5976.4 \pm 6.1$ kJ/mol.

Activity-composition relations

The activity-composition relations for the phlogopite-eastonite join and their relationship to chemical potential can be expressed by

$$\mu_i = \mu_i^0 + \text{R}T\ln a_i = \mu_i^0 + \Delta\bar{h}_{\text{mix},i} - \text{T}\Delta\bar{s}_{\text{mix},i} \quad (15)$$

where μ_i^0 is the chemical potential, a_i is the activity, and $\Delta\bar{h}_{\text{mix},i}$ and $\Delta\bar{s}_{\text{mix},i}$ are the partial molar enthalpy and entropy of mixing of the pure end-member in a solid solution. Thus, the activity of the end-member is

$$a_i = \exp[(\Delta\bar{h}_{\text{mix},i} - \text{T}\Delta\bar{s}_{\text{mix},i})(\text{R}T)^{-1}]. \quad (16)$$

The enthalpy of mixing of the phlogopite-eastonite join was defined in Equation 3, and the entropy of mixing is defined as

$$\Delta S_{\text{mix}} = S_{\text{conf}}^{\text{ss}} - (X_{\text{Phl}}S_{\text{conf}}^{\text{Phl}} + X_{\text{East}}S_{\text{conf}}^{\text{East}}). \quad (17)$$

The partial molar quantity of an extensive thermodynamic property Q is defined as

$$\bar{Q}_A = Q - X_B\,\text{d}Q/\text{d}X_B \quad (18)$$

where $\bar{Q}_A$ is the partial molar quantity of Q (in this case the enthalpy or entropy of mixing) for end-member A and X_B is the mole fraction of the end-member B. A similar expression can be written for $\bar{Q}_B$. The partial molar enthalpies of mixing for phlogopite and eastonite (in J/mol), derived from Equations 3 and 18, are

$$\begin{aligned}\Delta\bar{h}_{\text{mix,Phl}} &= X_{\text{East}}^2[(2W_{\text{East}}^H - W_{\text{Phl}}^H) + 2X_{\text{East}}(W_{\text{Phl}}^H - W_{\text{East}}^H)] \\ &= X_{\text{East}}^2[-65420 + 131\,720X_{\text{East}}] \end{aligned} \quad (19)$$

and

$$\begin{aligned}\Delta\bar{h}_{\text{mix,East}} &= (1 - X_{\text{East}})^2[(2W_{\text{Phl}}^H - W_{\text{East}}^H) + 2(1 - X_{\text{East}})(W_{\text{East}}^H - W_{\text{Phl}}^H)] \\ &= (1 - X_{\text{East}})^2[132\,160 - 131\,720(1 - X_{\text{East}})]. \end{aligned} \quad (20)$$

Similarly, the partial molar entropies of mixing (in J/mol·K), derived from Equations 13, 14, 17, and 18, are

$$\Delta\bar{s}_{\text{mix,Phl}} = -\text{R}\ln[27(1 - X_{\text{East}})^3(1 + X_{\text{East}})\cdot(3 - X_{\text{East}})^{-3}] \quad (21)$$

and

$$\Delta\bar{s}_{\text{mix,East}} = -\text{R}\ln[X_{\text{East}}(1 + X_{\text{East}})^2(3 - X_{\text{East}})^{-2}]. \quad (22)$$

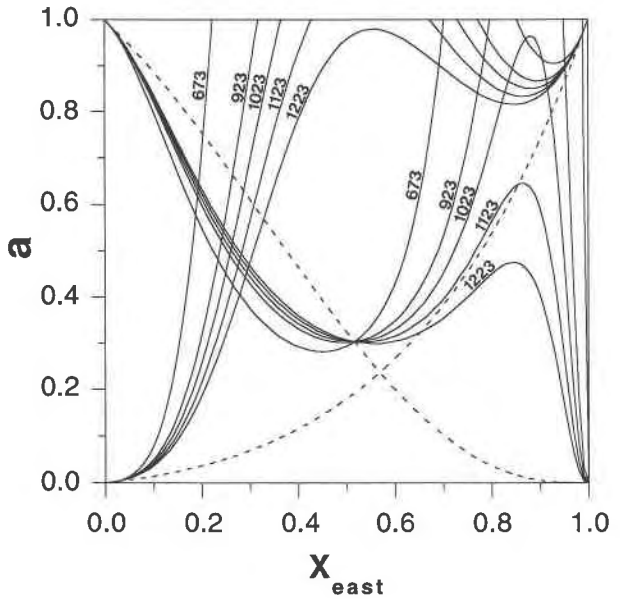

Fig. 4. Calculated activity-composition relations for the phlogopite-eastonite solid solution, assuming a short-range ordered distribution for the T-site configurational entropy. Dashed curves represent activities calculated assuming $\Delta H_{mix} = 0$. Solid curves represent calculated activities at T = 673, 923, 1023, 1123, and 1223 K. Curves for 673 and 923 K bracket sample synthesis temperatures.

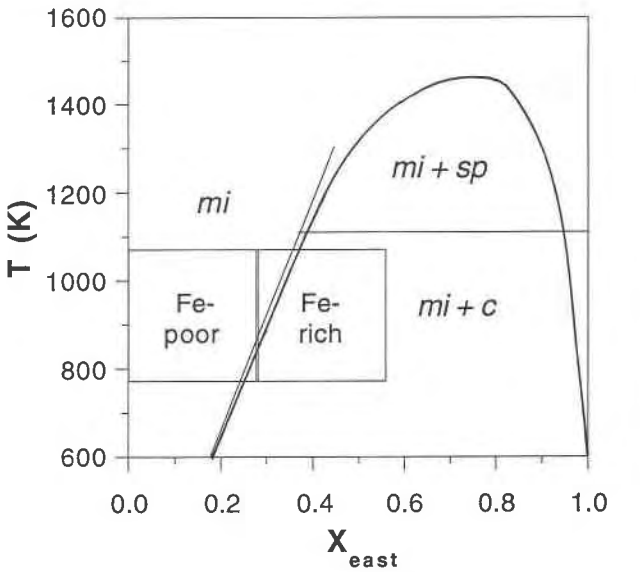

Fig. 5. Calculated position of the solvus for the phlogopite-eastonite join (curve). Labeled T-X fields bounded by lines represent observed synthesis products containing only mica (mi) at low X_{East}, mica and $MgAl_2O_4$ spinel (mi + sp) at high X_{East} and high temperature, or mica and corundum (mi + c) at high X_{East} and low temperature (Circone et al., 1991). Boxed areas represent observed ranges of [6,4]Al substitution in naturally occurring phlogopite and biotite from subamphibolite to granulite facies metamorphic assemblages (Guidotti, 1984). Fe-poor and Fe-rich fields correspond to micas with Fe/(Fe + Mg) ratios of <0.1 and >0.1, respectively.

Using these equations and Equation 16, the activities of the phlogopite-eastonite join were calculated for a range of temperatures (Fig. 4). The large, positive enthalpy of mixing and the difference in magnitude between the excess mixing parameters result in $a_{East} \gg 1$ over a large range of X_{East} and $a_{Phl} > 1$ at large values of X_{East}. Since the entropy of mixing is smaller for the random and ordered T-site models (Fig. 3), the ranges of X_{East} over which the activities are greater than 1 would be extended using either model. The calculated variations in activity predict a large region of immiscibility for the phlogopite-eastonite join. The position of the solvus can be determined from curves of Gibbs free energy of mixing, where

$$\Delta G_{mix} = \Delta H_{mix} - T\Delta S_{mix} = X_{Phl}\, RT \ln a_{Phl} + X_{East}\, RT \ln a_{East}. \quad (23)$$

The position of the solvus is located at the tangents to the Gibbs free energy of mixing curves at different temperatures. At these tangents the activities of phlogopite in the Mg,Si-rich and Al-rich solid solutions are equal, as are the activities of eastonite.

The predicted region of immiscibility (Fig. 5) contradicts the apparent range of solid solution observed at the mica synthesis temperatures (673–923 K). Either the synthesis products (mica ± corundum) do not represent the equilibrium assemblage or the synthetic samples consist of two exsolved micas. The latter possibility is ruled out for the following reasons. First, a sample synthesized at 923 K from a gel with the composition $Phl_{50}East_{50}$ would consist of two micas: 70% with $X_{East} \approx 0.32$ and 30% with $X_{East} \approx 0.96$. The lateral dimensions in the a-b crystallographic plane of these two micas would be significantly different (Circone et al., 1991) such that a single (hkl) reflection would be resolved into two peaks (e.g., 060, $\bar{1}32$-201, 202 are separated by 0.30, 0.15, 0.12° 2θ, respectively). However, the powder X-ray diffraction patterns do not show peak splitting or sufficient peak broadening to indicate the presence of exsolved mica. Second, the products from synthesis experiments performed between 673–1273 K and 1.0–8.3 kbar (Circone et al., 1991) are consistent with the calculated position of the phlogopite-rich limb of the solvus (Fig. 5). In the synthesis experiments, gel starting materials with low X_{East} produce a single mica phase. At higher X_{East} contents, synthesis products contain predominantly a single mica phase, plus an Al-rich phase ($MgAl_2O_4$ spinel > 1150 K, corundum < 1150 K), identified optically and by X-ray diffraction. The compositions (determined by electron microprobe analysis of individual platelets) of the synthetic micas coexisting with spinel are shifted to lower X_{East} contents corresponding to the phlogopite-rich limb of the solvus, and there is no evidence for a coexisting Al-rich mica. If the platelets that were probed consisted of a finely exsolved two-mica phase, the average composition would be shifted to a higher [6,4]Al content than is measured. Third, the nonzero enthalpies of mixing argue against the products being two-phase mixtures, whose enthalpies would vary linearly with composition.

TABLE 5. Thermodynamic data used to calculate phlogopite dehydration equilibria

Compound	$\Delta H^0_{f,298}$ (kJ/mol)	S^0_{298} (J/mol·K)	V^0_{298} (J/bar)
$KMg_3(AlSi_3)O_{10}(OH)_2$	−6211.73(564)[A]	331.78(100)[A,B]	14.967(1)[C]
	−6214.07(613)[D]		
	−6217.7[E]		
	−6215.7[F]		
	−6224.0[G]		
$K(Mg_2Al)(Al_2Si_2)O_{10}(OH)_2$	−6352.23(839)[A]	317.45(120)[A]	14.738(9)[C]
	−6363.04(602)[A]		
SiO_2	−910.70(100)	41.46(20)	2.269(0)
$KAlSi_3O_8$	−3959.56(337)	232.90(48)	10.905(10)
$MgSiO_3$	−1547.20(252)[H]	66.27(10)[I]	3.132(1)[I]
$MgAl_2O_4$	−2299.32(75)	80.63(42)	3.971(3)
H_2O(v)	−241.81(4)	188.83(4)	

Note: Data from Robie et al. (1978), except where noted. Numbers in parentheses are uncertainties in the last significant figures.
[A] This study.
[B] The entropy is 327.43(100) J/mol·K (assuming an ordered Al,Si distribution) and 334.60(100) J/mol·K (assuming a random Al,Si distribution).
[C] Circone et al. (1991).
[D] Clemens et al. (1987), recalculated (see text).
[E] Bohlen et al. (1983); $a_{H_2O} = 0.42$.
[F] Bohlen et al. (1983); $a_{H_2O} = 0.52$.
[G] Peterson and Newton (1989).
[H] Brousse et al. (1984).
[I] Krupka et al. (1985a).

Instead, what is unusual is the observed trend of increasing [6,4]Al solubility in phlogopite with decreasing synthesis temperature (Robert, 1976; Circone et al., 1991). This appears inconsistent with the thermodynamics of mixing, since the range of solid solution should increase with increasing temperature (Fig. 5). We surmise that, at the low temperatures of synthesis, mica growth from the homogeneous gel starting materials produced phlogopite with a high, metastable [6,4]Al content in place of the predicted equilibrium assemblage of two-mica solid solutions.

Furthermore, the [6,4]Al solubility in phlogopite predicted from the activity-composition relationships is consistent with the observed compositional range of naturally occurring trioctahedral micas from metamorphic assemblages. In natural Fe-poor, Al-rich phlogopite, [6]Al contents are limited to ≤ 0.30 per three octahedral sites (e.g., Guidotti, 1984, Fig. 35). Since [6]Al is in part charge balanced by [4]Al in natural phlogopite, the actual fraction of [6,4]Al substitution in the natural micas would be slightly less than 0.30. The calculated position of the solvus between 773 and 1073 K (representing the temperature range for sub-amphibolite to granulite-grade metamorphic conditions) in Figure 5 is consistent with the composition of natural Fe-poor phlogopite formed under these conditions. If Fe is added to the system and ideal mixing between Fe and Mg is assumed, the entropy of mixing term will increase, the size of the solvus will be reduced, and the upper limit of [6,4]Al substitution will increase with increasing Fe content, which is consistent with the observed compositional trends in natural phlogopite and biotite (Guidotti, 1984). The measured and calculated thermodynamic properties of magnesium aluminum phlogopite are applied to phlogopite equilibria in the next section.

THE EQUILIBRIUM PHLOGOPITE + 3 QUARTZ = SANIDINE + 3 ENSTATITE + H_2O VAPOR

The P,T position of the equilibrium of Reaction 1 has been calculated to assess the thermodynamic data obtained in this study and to illustrate the effect of [6,4]Al content on the stability of phlogopite in the presence of quartz. The P,T equilibria of dehydration reactions involving phlogopite are extremely sensitive to small uncertainties in the thermodynamic data (Clemens et al., 1987). We will illustrate these uncertainties by focusing on the shift in the equilibrium position as a function of (1) the enthalpy of formation of phlogopite, (2) the entropy model for the T sites, and (3) the estimated heat capacity of eastonite. It is not our intent, however, to analyze the available thermodynamic and phase equilibria data for phlogopite to derive a definitive set of thermochemical data. That endeavor was not our primary goal and is beyond the scope of this study.

The equilibrium P,T position of Reaction 1 was calculated using

$$\Delta G_r = 0 = \Delta H^0_{r,298} - T\,\Delta S^0_{r,298} + \int_{298}^{T} \Delta C_{P,r}\,dT - T\int_{298}^{T} \frac{\Delta C_{P,r}}{T}\,dT + \Delta V^0_{r,298}\left[1 + \Delta\alpha(T - 298)P - \frac{\Delta\beta}{2}P^2\right] + RT \ln f_{H_2O} \quad (24)$$

where the subscript r denotes the sum of the products minus the sum of the reactants in Reaction 1. The thermodynamic data used in the calculations are summarized in Table 5. The standard-state entropy of sanidine assumes complete Al,Si disorder. The heat capacities for all

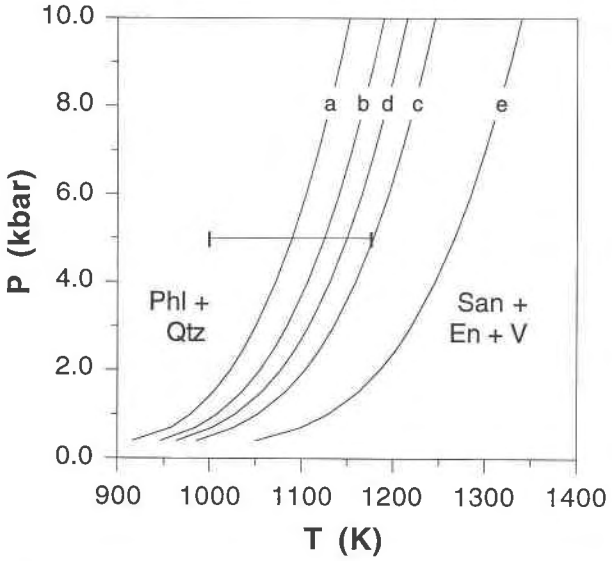

Fig. 6. Calculated P,T position of Reaction 1 using different $\Delta H^0_{f,298}$ of phlogopite from various sources. All curves are calculated from the thermodynamic data in Table 5 and assume the short-range order model for the T-site configurational entropy of phlogopite. Curve a = $\Delta H^0_{f,298}$ for phlogopite from this study. Bracket represents the 5.6 kJ/mol uncertainty in $\Delta H^0_{f,298}$. Curve b = $\Delta H^0_{f,298}$ from Clemens et al. (1987). Curve c = $\Delta H^0_{f,298}$ calculated from the phase equilibria experiments of Bohlen et al. (1983), with the assumption that $\gamma_{H_2O} = 1.2$ and $a_{H_2O} = 0.42$. Curve d: As in curve c, but $\gamma_{H_2O} = 1.5$ and $a_{H_2O} = 0.52$ is assumed. Curve e = $\Delta H^0_{f,298}$ calculated from the phase equilibria experiments of Peterson and Newton (1989).

phases are from Robie et al. (1978), except for phlogopite (Robie and Hemingway, 1984) and orthoenstatite (Krupka et al., 1985b). The f_{H_2O} data are from Burnham et al. (1969). The mineral compressibilities (β) and thermal expansivities (α) are from the data set of Holland and Powell (1990) and references therein. All calculations assume $P_{H_2O} = P_{tot}$.

The enthalpy of formation of phlogopite can also be calculated from the phase equilibria results of Bohlen et al. (1983) and of Peterson and Newton (1989). Bohlen et al. bracketed Reaction 1 reversibly at 1053–1073 K, 5.0 kbar in the presence of an H_2O-CO_2 fluid phase with $X_{H_2O} = 0.35$. Peterson and Newton (1989, Fig. 5) determined the position of Reaction 1 from several experiments over the P,T range 0.30–0.49 kbar, 750–795 °C. They concluded that the invariant point involving the intersection of Reaction 1 with the solidus lies at 790–795 °C, 0.44–0.50 kbar, in agreement with Montana and Brearley (1989). The $\Delta H^0_{f,298}$ of phlogopite (Table 5) were calculated assuming a short-range ordered distribution of Al and Si on T sites. For the reversal of Bohlen et al. (1983), an activity coefficient of H_2O (γ_{H_2O}) between 1.2 ($a_{H_2O} = 0.42$) and 1.5 ($a_{H_2O} = 0.52$) was used. This represents the expected range of deviation from ideality of the fluid mixture.

The P,T equilibrium position of Reaction 1 has been calculated using the values for $\Delta H^0_{f,298}$ of phlogopite in Table 5 (Fig. 6). Curves a and b, based on $\Delta H^0_{f,298}$ of phlogopite determined from high-temperature solution calorimetry data, are ~35 K apart at 5.0 kbar. Curves c and d, based on $\Delta H^0_{f,298}$ of phlogopite from the phase equilibria data of Bohlen et al. (1983), are ~30 K apart at 5.0 kbar and represent the uncertainty arising from the estimated range of γ_{H_2O}. Curve e, based on $\Delta H^0_{f,298}$ of phlogopite from the phase equilibria data of Peterson and Newton (1989), lies at significantly higher temperatures. The calorimetric data from this study and from Clemens et al. (1987) are in closest agreement with the results of Bohlen et al. (1983). The bracket on curve a, which spans ~175 K at 5.0 kbar, represents only the uncertainty in $\Delta H^0_{f,298}$ from this study. Curves a, b, c, and d are equivalent within the propagated errors of the calorimetric data sets. The uncertainties in the $\Delta H^0_{f,298}$ obtained from phase equilibria experiments were assessed to be ~6 kJ/mol by Clemens et al. (1987).

The curves shown in Figure 6 were calculated using the short-range order Al,Si distribution model. The positions of curves c, d, and e are not affected significantly if either the random or ordered T-site model is assumed for the calculations because the Gibbs free energy is measured directly and $\Delta H^0_{f,298}$ will compensate any changes in S^0_{298}. At 5.0 kbar the curves shift less than ±10 K for either model, and $\Delta H^0_{f,298}$ remains within the uncertainties quoted in Table 5. However, the positions of curves a and b are affected significantly by the T-site entropy model used. Both curves shift approximately +50 K if one assumes a random distribution and −70 K if one assumes an ordered model, but they remain within the bracketed uncertainties for the $\Delta H^0_{f,298}$ of phlogopite.

The P,T position of Reaction 1 was then calculated for magnesium aluminum phlogopite with varying [6,4]Al content (Fig. 7) using the reaction

$$K(Mg_{3-X_{East}}Al_{X_{East}})(Al_{1+X_{East}}Si_{3-X_{East}})O_{10}(OH)_2 + (3 - X_{East})SiO_2 = KAlSi_3O_8 + (3 - 2X_{East})MgSiO_3 + X_{East}MgAl_2O_4 + H_2O. \quad (25)$$

Calculations were made using $\Delta H^0_{f,298}$ of phlogopite from this study, the estimated heat capacity of eastonite from Berman and Brown (1985) and the activity-composition relations defined in Equations 16, 19, 20, 21, and 22. The equilibrium position of Reaction 25 shifts to higher temperatures with increasing [6,4]Al content of phlogopite, suggesting that phlogopite is stabilized by the [6,4]Al substitution. This trend of increasing mica stability with increasing [6,4]Al content was observed by Rutherford (1973) for the annite-siderophyllite join. In these phase equilibria experiments, the breakdown reaction of an annite sample with starting composition An_{75} was shifted up >100 K at constant P (up 170 K along the QFM buffer position in T − log f_{O_2} space) relative to that of the end-member annite.

The uncertainty in the heat capacity of eastonite is less significant than the uncertainties in the $\Delta H^{\circ}_{f,298}$ of phlogopite and eastonite. As discussed previously, the heat content and entropy of eastonite at the temperatures of reaction are probably higher than those estimated using the heat capacity model of Berman and Brown (1985). Reaction 25 was recalculated using their model and assuming a +3.2% correction for the heat content and +1.6% correction for the entropy, based on the heat capacity results for the magnesium aluminum phlogopite samples in this study. At 5.0 kbar, the curves calculated for X_{East} = 0.05, 0.10, and 0.15 are shifted up approximately 7, 15, and 20 K, respectively.

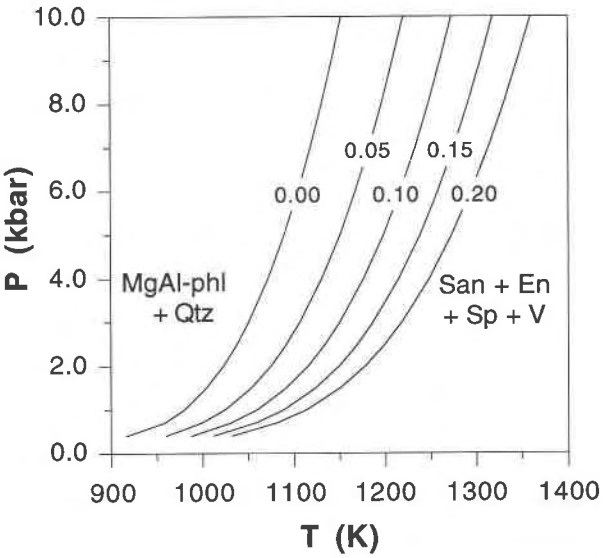

Fig. 7. Calculated P,T positions of Reaction 25 for different values of X_{East} (labels on curves) using the $\Delta H^{\circ}_{f,298}$ for phlogopite from this study, $\Delta H^{\circ}_{f,298}$ = −6352.2 ± 8.4 kJ/mol for eastonite, the estimated C_P of eastonite (Berman and Brown, 1985), and the short-range order model for the T-site configurational entropy.

Conclusions

The results from this study and Clemens et al. (1987) agree within the uncertainties of the calorimetric data with the phase equilibria results of Bohlen et al. (1983), yielding a value of $\Delta H^{\circ}_{f,298}$ = −6215.0 ± 3.5 kJ/mol. The phase equilibria results of Peterson and Newton (1989) differ significantly, yielding $\Delta H^{\circ}_{f,298}$ = −6224.0 kJ/mol. Both sources of data have some limitations. Although the uncertainties in the calorimetric data are reasonable, considering the large molecular weight of the micas, they produce large uncertainties in the calculation of dehydration equilibria of phlogopite. The large formula weights and large enthalpies of solution of the micas impose a limit to the precision of the calorimetry technique. This is similarly true for amphiboles (e.g., Graham and Navrotsky, 1986). The uncertainties related to modeling the Al,Si distribution in the tetrahedral sites are less significant. The enthalpy of formation of eastonite also is subject to the uncertainty in its heat capacity, and a measured heat capacity of synthetic eastonite is needed to better constrain the $\Delta H^{\circ}_{f,298}$. Phase equilibria experiments on mica dehydration are also beset with uncertainties. In the experiments of Bohlen et al. (1983), the fluid mixing properties are ill constrained at the geologically relevant pressures and temperatures. Furthermore, the persistence of metastable mica synthesis products, evidenced by the synthesis of Al-rich phlogopite in the region of immiscibility for the phlogopite-eastonite join, attests to the sluggishness of mica reaction and limits the accuracy of phase equilibria experiments performed at low temperatures and pressures. The discrepancies among published data sets (e.g., Montana and Brearley, 1989) suggest that the phase equilibria experiments are not without problems. Some phase equilibria studies (e.g., Bohlen et al., 1983; Montana and Brearley, 1989) have suggested that varying degrees of Al,Si ordering in synthetic and natural micas may contribute to these experimental discrepancies; however, ^{29}Si MAS NMR spectroscopic studies (e.g., Herrero et al., 1985a, 1985b, 1987; Circone et al., 1991) have not produced evidence for different degrees of ordering in samples with comparable [4]Al/[4](Al + Si) ratios. Furthermore, mica polytypism (*1Md* vs. *1M*) does not contribute significantly to either the enthalpy of formation or to the entropy (based on infrared and Raman spectroscopy) of phlogopite (Clemens et al., 1987). The source of the observed discrepancies in the phase equilibria data must arise from other sources. The fact that one can prepare solid solutions that may be metastable with respect to unmixing and decomposition to other assemblages is an asset, rather than a liability, when using solution calorimetry techniques to define the thermodynamics of a system. Once such metastable phases are characterized structurally and energetically, the extent of their stability or metastability can be deduced.

Nonetheless, we have characterized the subregular solution behavior of the phlogopite-eastonite join and predicted the increase in stability of phlogopite with increasing [6,4]Al content based on solution calorimetry data for a series of well-characterized synthetic magnesium aluminum phlogopite samples. The large, positive, asymmetric enthalpy of mixing for the solid solution and the calculated activity-composition relations predict a large region of immiscibility between phlogopite and eastonite that is consistent with the compositions of Fe-poor trioctahedral micas in natural assemblages.

Acknowledgments

This work was supported by the U.S. Department of Energy (grant DE-FG02-85ER-13437). We thank Papu Maniar for collecting and fitting the heat capacity data. We thank W. Lamb and an anonymous reviewer for their constructive reviews.

References cited

Akaogi, M., and Navrotsky, A. (1984) The quartz-coesite-stishovite transformations: New calorimetric measurements and calculation of phase diagrams. Physics of the Earth and Planetary Interiors, 36, 124–134.

Bailey, S.W. (1984) Crystal chemistry of the true micas. In Mineralogical Society of America Reviews in Mineralogy, 13, 13–57.

Berman, R.G., and Brown, T.H. (1985) Heat capacity of minerals in the system Na_2O-K_2O-CaO-MgO-FeO-Fe_2O_3-Al_2O_3-SiO_2-TiO_2-H_2O-CO_2: Representation, estimation, and high temperature extrapolation. Contributions to Mineralogy and Petrology, 89, 168–183.

Bohlen, S.R., Boettcher, A.L., Wall, V.J., and Clemens, J.D. (1983) Stability of phlogopite-quartz and sanidine-quartz: A model for melting in the lower crust. Contributions to Mineralogy and Petrology, 83, 270–277.

Brousse, C., Newton, R.C., and Kleppa, O.J. (1984) Enthalpy of formation of forsterite, enstatite, akermanite, monticellite and merwinite at 1073 K determined by alkali borate solution calorimetry. Geochimica et Cosmochimica Acta, 48, 1081–1088.

Burnham, C.W., Holloway, J.R., and Davis, N.F. (1969) Thermodynamic properties of water to 1,000 °C and 10,000 bars. Geological Society of America Special Paper 132, 96 p.

Circone, S., Navrotsky, A., Kirkpatrick, R.J., and Graham, C.M. (1991) Substitution of [6,4]Al in phlogopite: Mica characterization, unit-cell variation, ^{27}Al and ^{29}Si MAS-NMR spectroscopy, and Al-Si distribution in the tetrahedral sheet. American Mineralogist, 76, 1485–1501.

Clemens, J.D., Circone, S., Navrotsky, A., McMillan, P.F., Smith, B.K., and Wall, V.J. (1987) Phlogopite: High temperature solution calorimetry, thermodynamic properties, Al-Si and stacking disorder, and phase equilibria. Geochimica et Cosmochimica Acta, 51, 2569–2578.

Davies, P.K., and Navrotsky, A. (1981) Thermodynamics of solid solution formation in NiO-MgO and NiO-ZnO. Journal of Solid State Chemistry, 38, 264–276.

Graham, C.M., and Navrotsky, A. (1986) Thermochemistry of the tremolite-edenite amphiboles using fluorine, analogues, and applications to amphibole-plagioclase-quartz equilibria. Contributions to Mineralogy and Petrology, 93, 18–32.

Guggenheim, S. (1984) The brittle micas. In Mineralogical Society of America Reviews in Mineralogy, 13, 61–104.

Guidotti, C.V. (1984) Micas in metamorphic rocks. In Mineralogical Society of America Reviews in Mineralogy, 13, 357–467.

Helgeson, H.C., Delaney, J.M., Nesbitt, H.W., and Bird, D.K. (1978) Summary and critique of the thermodynamic properties of rock-forming minerals. American Journal of Science, 278A, 1–229.

Herrero, C.P., Sanz, J., and Serratosa, J.M. (1985a) Si,Al distribution in micas: Analysis by high-resolution ^{29}Si NMR spectroscopy. Journal of Physics C: Solid State Physics, 18, 13–22.

——— (1985b) Tetrahedral cation ordering in layer silicates by ^{29}Si NMR spectroscopy. Solid State Communications, 53, 151–154.

Herrero, C.P., Gregorkiewitz, M., Sanz, J., and Serratosa, J.M. (1987) ^{29}Si MAS-NMR spectroscopy of mica-type silicates: Observed and predicted distribution of tetrahedral Al-Si. Physics and Chemistry of Minerals, 15, 84–90.

Hewitt, D.A., and Wones, D.R. (1975) Physical properties of some synthetic Fe-Mg-Al trioctahedral biotites. American Mineralogist, 60, 854–862.

Holland, T.J.B., and Powell, R. (1990) An enlarged and updated internally consistent thermodynamic data set with uncertainties and correlations: The system K_2O-Na_2O-CaO-MgO-MnO-FeO-Fe_2O_3-Al_2O_3-TiO_2-SiO_2-C-H-O_2. Journal of Metamorphic Geology, 8, 89–124.

Kiseleva, I.A., and Ogorodova, L.P. (1984) High-temperature solution calorimetry for determining the enthalpies of formation for hydroxyl-containing minerals such as talc and tremolite. Geochemistry International, 21, 36–46.

Krupka, K.M., Robie, R.A., Hemingway, B.S., Kerrick, D.M., and Ito, J. (1985a) Low-temperature heat capacities and derived thermodynamic properties of anthophyllite, diopside, enstatite, bronzite, and wollastonite. American Mineralogist, 70, 249–260.

Krupka, K.M., Hemingway, B.S., Robie, R.A., and Kerrick, D.M. (1985b) High-temperature heat capacities and derived thermodynamic properties of anthophyllite, diopside, dolomite, enstatite, bronzite, talc, tremolite, and wollastonite. American Mineralogist, 70, 261–271.

Livi, K.J.T., and Veblen, D.R. (1987) Eastonite: From Easton, Pennsylvania: A mixture of phlogopite and a new form of serpentine. American Mineralogist, 72, 113–125.

Montana, A., and Brearley, M. (1989) An appraisal of the stability of phlogopite in the crust and in the mantle. American Mineralogist, 74, 1–4.

Mueller, R.F. (1972) Stability of biotite: A discussion. American Mineralogist, 57, 300–316.

Navrotsky, A. (1977) Progress and new directions in high temperature calorimetry. Physics and Chemistry of Minerals, 2, 89–104.

——— (1987) Models of crystalline solutions. In Mineralogical Society of America Reviews in Mineralogy, 17, 35–69.

Navrotsky, A., Wechsler, B.A., Geisinger, K., and Seifert, F. (1986) Thermochemistry of $MgAl_2O_4$-$Al_{8/3}O_4$ defect spinels. Journal of the American Ceramic Society, 69, 418–422.

Peterson, J.W., and Newton, R.C. (1989) Reversed experiments on biotite-quartz-feldspar melting in the system KMASH: Implications for crustal anatexis. Journal of Geology, 97, 465–485.

Rapp, R.P., and Navrotsky, A. (1990) Refinement of heats of solution of common mineral-forming oxides via thermochemical cycles of carbonates and hydroxides. Eos, 71, 1648.

Richet, P., Bottinga, Y., Denielou, L., Petitet, J.P., and Tequi, C. (1982) Thermodynamic properties of quartz, cristobalite and amorphous SiO_2: Drop calorimetry measurements between 1000 and 1800 K and a review from 0 to 2000 K. Geochimica et Cosmochimica Acta, 46, 2639–2658.

Robert, J.-L. (1976) Phlogopite solid solutions in the system K_2O-MgO-Al_2O_3-SiO_2-H_2O. Chemical Geology, 17, 195–212.

Robie, R.A., and Hemingway, B.S. (1984) Heat capacities and entropies of phlogopite ($KMg_3[AlSi_3O_{10}](OH)_2$) and paragonite ($NaAl_2[AlSi_3O_{10}](OH)_2$) between 5 and 900 K and estimates of the enthalpies and Gibbs free energies of formation. American Mineralogist, 69, 858–868.

Robie, R.A., Hemingway, B.S., and Fisher, J.R. (1978) Thermodynamic properties of minerals and related substances at 298.15 K and 1 bar (10^5 pascals) pressure and at higher temperatures. U.S. Geological Survey Bulletin, 1452, 456 p.

Robinson, G.R., and Haas, J.L. (1983) Heat capacity, relative enthalpy, and calorimetric entropy of silicate minerals: An empirical method of prediction. American Mineralogist, 68, 541–553.

Rutherford, M.J. (1973) The phase relations of aluminous iron biotites in the system $KAlSi_3O_8$-$KAlSiO_4$-Al_2O_3-Fe-O-H. Journal of Petrology, 14, 159–180.

Sanz, J., and Serratosa, J.M. (1984) ^{29}Si and ^{27}Al high-resolution MAS-NMR spectra of phyllosilicates. Journal of the American Chemical Society, 106, 4790–4793.

Vedder, W., and Wilkins, R.W.T. (1969) Dehydroxylation and rehydroxylation, oxidation and reduction of micas. American Mineralogist, 54, 482–507.

Wones, D.R. (1972) Stability of biotite: A reply. American Mineralogist, 57, 316–317.

Wones, D.R., and Eugster, H.P. (1965) Stability of biotite: Experiment, theory, and application. American Mineralogist, 50, 1228–1272.

Manuscript received August 8, 1991
Manuscript accepted July 16, 1992

Appendix 1. Additional evidence for the validity of lead borate calorimetry on hydrous phases

In calorimetric studies involving hydrous phases (Kiseleva and Ogorodova, 1984; Clemens et al., 1987; this study), the reproducible dissolution of these phases in molten lead borate must be ascertained in two contexts. First, for the measured enthalpies of mixing of a solid solution to be valid, one must make sure that there is no unexpected interaction among the various components (oxides and H_2O) reacting with the solvent. This has been confirmed by the following. (1) The measured enthalpies of solution for a sample are not affected by the presence of previously dissolved species from one or two calorimetry experiments on micas with the same or different composition. (2) For a wide range of sample weights (6–28 mg), the measured en-

thalpy of solution or drop solution is independent of the amount of sample dissolved. (3) The ΔH_{soln} for the mica with $X_{East} = 0.45$ measured using the drop solution cycle (277.1 kJ/mol, based on two drop solution and three transposed temperature drop experiments) is within 1 sd of the direct solution data (Table 2), indicating that the two methods for obtaining ΔH_{soln} are internally consistent. (4) The enthalpies of solution of equimolar mechanical mixtures of samples with $X_{East} = 0.00$ and 0.45 (280.8 kJ/mol, based on two solution measurements) and with $X_{East} = 0.00$ and 0.92 (277.8 kJ/mol, based on six drop solution measurements) are equal to the weighted averages of the enthalpies of solution of their end-members (275.5 ± 6.5 and 277.5 ± 8.4 kJ/mol, respectively). These observations suggest infinite dilute solution behavior of magnesium aluminum phlogopite in molten lead borate, indicating that the observed deviation of the solution data from ideal mixing results from the nonideal behavior of the phlogopite-eastonite solid solution and not from any complex behavior of dissolved species in the melt. Thus, we conclude that the present calorimetric methodology allows us to measure accurately heats of mixing resulting from coupled ionic substitutions in a phase having constant H_2O content. A similar conclusion was drawn by Graham and Navrotsky (1986) for the mixing properties of fluoramphiboles and by A. Pawley (unpublished data) for hydroxyamphiboles.

Second, one must confirm that the final state of H_2O is sufficiently well characterized to allow calculation of enthalpies of formation of hydrous phases from reactants having different H_2O contents, e.g., brucite or H_2O itself. A set of experiments that achieve this goal is described separately (Rapp and Navrotsky, 1990; Navrotsky et al., unpublished data, 1992). Here we summarize only the points relevant to the present study. (1) The calorimetry experiments of Kiseleva and Ogorodova (1984), Clemens et al. (1987), and this study, all performed in a static air atmosphere near 973 K, indicate that H_2O derived from brucite and portlandite appears to interact with the lead borate melt with an exothermic enthalpy in the range −24 to −27 kJ/mol of H_2O introduced. However, both weight change experiments and the occasional observation of traces of H_2O condensed in the calorimeter glassware assembly suggest that all the H_2O does not remain dissolved. The consistency of the data and the independence of the measured enthalpy of reaction from the mass of the sample suggest that a reproducible and kinetically controlled fraction of the H_2O is in solution, resulting in a reproducible but not completely characterized final state. (2) Under conditions of flowing atmosphere (1–2 cc/s of air or Ar), the observed enthalpy of interaction of H_2O with molten lead borate, based on experiments involving $Ca(OH)_2$, $Mg(OH)_2$, $Cu(OH)_2$, and NaOH (Navrotsky et al., unpublished data, 1992), is 0 ± 5 kJ/mol of H_2O added. Weight change experiments and direct chemical analysis of the lead borate glass show that less than 1% of the H_2O added remains in the solvent. The calorimetric experiments returned to the original baseline better than those in static air did. (3) Drop solution and solution calorimetry have been performed, respectively, on brucite and phlogopite (the same used in the present study) in a flowing Ar atmosphere. The measured ΔH_{soln} at 977 K are 66.1 ± 4.0 and 302.0 ± 1.8 kJ/mol, respectively. The enthalpy of formation of phlogopite calculated using Equation 4 and the data obtained in flowing atmosphere is −6217.18 ± 6.40 kJ/mol, identical within the experimental uncertainties to that using the data obtained in static atmosphere. We conclude that, although the flowing atmosphere technique is to be preferred for future work because it produces a better characterized final state, the present data on enthalpies of formation for the phlogopite-eastonite join are valid.

Appendix 2. Statistical model for the configurational entropy of the T sites

The expression for the configurational entropy arising from Al and Si mixing on a linear array of tetrahedra is derived in the following way. Equation 10 defined the configurational entropy for the random mixing of N_A A atoms and N_B B atoms, where

$$\Omega = \frac{(N_A + N_B)!}{N_A! N_B!} \tag{A1}$$

is the number of permutations of $(N_A + N_B)$ atoms, excluding the indistinguishable permutations in which identical atoms are interchanged. If we assume that A-A combinations are not allowed, then the number of permutations is significantly reduced. In order to eliminate A-A combinations, one B atom is placed after each A atom, and we calculate the number of permutations of B atoms (boldfaced) mixing with AB units, producing a string of atoms such as:

$$AB\mathbf{B}ABABAB\mathbf{BB}ABAB \ldots BAB\mathbf{B}AB\mathbf{B}ABAB\mathbf{BB}AB.$$

The permutations which would have ABB are indistinguishable from ABB. Since the last A atom in the string does not need a B atom after it, the number of AB units is N_A and the number of B atoms that are free to mix is $N_B - (N_A - 1)$. Therefore, the number of permutations is

$$\Omega = \frac{[N_B - (N_A - 1) + N_A]!}{[N_B - (N_A - 1)]! N_A!} = \frac{(N_B + 1)!}{(N_B - N_A + 1)! N_A!}. \tag{A2}$$

If we assume that the last atom in the chain is never an A, then the number of B atoms free to mix is $N_B - N_A$, and the number of permutations simplifies to

$$\Omega = \frac{N_B!}{(N_B - N_A)! N_A!}. \tag{A3}$$

This expression results in a slight underestimation of the configurational entropy of the linear chain of tetrahedra; however, the simplification is justified because (1) the configurational entropy of the tetrahedral sheet is already overestimated by this one-dimensional model, since the possibility of A-A combinations between adjacent chains of tetrahedra are not considered, and (2) the approximation only becomes poor when $N_A \approx N_B$.

Thus, the configurational entropy for Al and Si mixing on a linear array of tetrahedra is

$$S_{conf}^{T,lin} = k \ln \frac{N_{Si}!}{(N_{Si} - N_{Al})! N_{Al}!} \tag{A4}$$

and with Stirling's approximation becomes

$$S_{conf}^{T,lin} = k\left[N_{Si} \ln \frac{N_{Si}}{(N_{Si} - N_{Al})} + N_{Al} \ln \frac{(N_{Si} - N_{Al})}{N_{Al}}\right] = -4R\left[X_T^{Si} \ln \frac{(X_T^{Si} - X_T^{Al})}{X_T^{Si}} - X_T^{Al} \ln \frac{(X_T^{Si} - X_T^{Al})}{X_T^{Al}}\right]. \tag{A5}$$

This expression can be rewritten in terms of X_{East} by substituting $X_T^{Al} = \frac{1}{4}(1 + X_{East})$ and $X_T^{Si} = \frac{1}{4}(3 - X_{East})$ into Equation A5, which becomes Equation 14.